Nov 3rd, 12:00 AM

Behavior and Design of Axially Compressed Sheathed Wall Studs

L. C. M. Vieira Jr.

B. W. Schafer

Twentieth International Specialty Conference on Cold-Formed Steel Structures
St. Louis, Missouri, U.S.A., November 3 & 4, 2010

Behavior and Design of Axially Compressed Sheathed Wall Studs

L.C.M. Vieira Jr.[1] and B.W. Schafer[2]

Abstract

The objective of this paper is to summarize efforts in a multi year project dedicated to developing a reliable design method for cold-formed steel wall studs that rely on sheathing for bracing. Testing on single columns with sheathing, and full-scale walls with sheathing, are summarized. Particular emphasis is placed on the observed limit states given the different sheathing conditions. The sheathing supplies beneficial restraint to the wall studs and the stiffness of this sheathing-based restraint is characterized experimentally and analytically. A unique application of the Direct Strength Method of design is explored where the sheathing-based restraint is used explicitly in determination of the elastic buckling loads of the wall studs, and then these elastic buckling loads are utilized to determine the strength. The test results are compared with the newly proposed design method as well as with previous design methods adopted by the AISI Specification. Good agreement is demonstrated for the new approach both in terms of strength and limit states prediction.

1 Introduction

Cold-formed steel walls have long relied on bracing to prohibit detrimental global buckling modes and to develop the full capacity of the wall. In the simplest case bracing is supplied by an explicit member, such as the bridging channel shown in Figure 1a. However, since at least the 1940s, the additional resistance supplied to a cold-formed steel stud due to its connection to sheathing, Figure 1b, has intrigued researchers and designers. Sheathing bracing offers the potential for significant economy since the sheathing is already supplied for the walls basic functioning. An isolated, but sheathed, column (wall stud) is shown in Figure 1c, and in this work tests were conducted on both

[1] Graduate Research Assistant, Johns Hopkins University, Baltimore, MD, USA
[2] Professor, Johns Hopkins University, Baltimore, MD, USA

isolated and full walls. It has been common in the past to simplify the role of the bracing of the column to an in-plane spring column model, as shown in Figure 1d. In this work, the stiffness provided by the sheathing is pursued for both in-plane and out-of plane restraint, as shown in Figure 1e, as it was found that each of these restraints play an important role in bracing the wall stud.

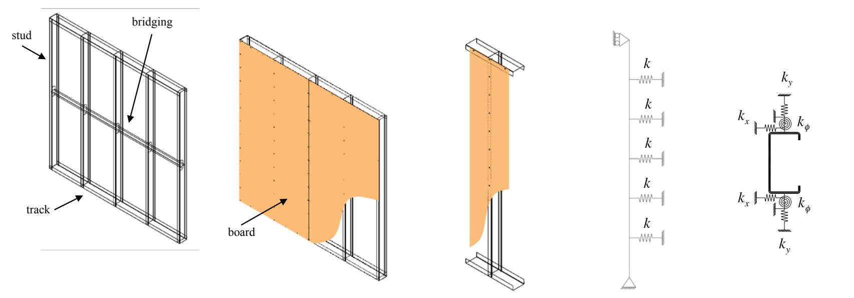

Figure 1 – Stud bracing

This paper summarizes the results of a larger project that aims to understand the behavior of sheathed wall studs and translate that knowledge into a reliable design method. The design method is corroborated by experimental tests. Single column tests, full wall tests, and rotational and translational stiffness tests were all conducted in support of the larger effort to develop a design method.

2 Experiments on sheathed studs and walls

The single column and full-scale sheathed wall tests summarized in this paper are covered in detail in progress reports: Shifferaw et al. (2009) and Vieira and Schafer (2009). The reports cover a series of thirteen full-scale walls and twenty-seven single columns all tested under axial compression. The studies concentrated on the impact of attaching different types of sheathing to the side of the wall, specifically bare (no sheathing), oriented strand board (OSB) or Gypsum (Gyp), under a variety of different combinations.

The cold-formed steel studs used in the test are 362S162-68's (50 ksi) (SSMA/ASTM nomenclature) throughout. Two types of sheathing are employed: OSB (7/16 in., rated 24/16, exposure 1) and Gypsum (½ in. Sheetrock). Number 6 screws (Simpson #6 x 1 5/8'') were used to connect to the Gypsum boards and number 8 screws (Simpson #8 x 1 15/16'') to connect to the OSB boards. The single column tests covered short (two feet), intermediate (four and six feet) and long columns (eight feet). The walls have five studs of 8 feet equally spaced between two tracks of the same length. The boards are connected to the studs every 6 inches at the edge studs of the walls and every 12 inches in the field studs of the walls and the single column tests.

2.1 Observed Strength

Strength and observed failure mode for the single column tests as a function of column length and sheathing type are summarized in Table 1. Not provided are a series of studies on the end boundary conditions (Shifferaw et al. 2009) that examine the impact of the track and the sheathing on the strength and failure mode. It was found that the sheathing should not be allowed to bear against the end platens of the test fixture or artifically high strength is observed.

For the full-scale wall tests, strength and observed failure mode are summarized in Table 2. Multiple tests are conducted on each nominally identical sheathing arrangement and the mean value is also reported. To compare the full-scale walls with the single column tests, the per stud strength (mean value divided by 5 studs) is reported. The results reveal that the attachment of boards to the side of the wall can increase the axial strength of the wall by as much as 91%, for example, when comparing the case of Bare-Bare to that of OSB-OSB. However, detrimental results were also observed; specifically, the OSB-Bare walls had no post-buckling reserve as they failed in a dramatic flexural-torsional mode. In walls with symmetric sheathing (OSB-OSB and Gyp-Gyp), the observed failure mode of the stud was local buckling, and exhibited deformations essentially identical for the two sheathing types. However, for the case with asymmetric sheathing (OSB-Gyp) local buckling failure modes as well as other failure modes (primarily distortional buckling) were also observed in the studs.

As expected the peak load follows in an ascending order of Bare-Bare, OSB-Bare, Gyp-Gyp, OSB-Gyp and OSB-OSB, with little exception. Comparing Table 1 to Table 2 the limit states are the same for 8 ft single column tests and the full 8 ft x 8 ft wall, nonetheless, the peak load is usually slightly lower in the wall tests, except for the OSB-Bare tests. This is somewhat surprising as it demonstrates that full sheathing resistance is developed even with only one line of vertical fasteners, as in the single column tests. Postulated reasons for the slight decrease in the full-scale wall tests, when compared with the single columns tests: (a) local buckling in the outermost studs of the wall do not always fully bear on the track since they are at the ends of the track (b) the tributary area of the board designated to each stud in the wall as engaged for sheathing resistance is modestly less than in the single column tests, (c) bracing forces in the sheathing accumulate and may have a modestly detrimental influence, (d) when the weakest of the 5 studs in the wall fail the forces must be carried by the other studs, thus observed strengths may be more of a weakest link strength as opposed to the idealized redistribution of a fully parallel system.

For the OSB-Bare case the failure is in flexural-torsional buckling and the full wall has a higher observed per stud mean strength than the single column, but the variability is significant and the failure mode in the full walls is dramatic and without any post-peak reserve.

Table 1 – Column tests, peak load and limit state

Length (feet)	Sheathing Configuration	Peak Load (kips)	Limit State
2	Bare-Bare	19.77	Distortional
	OSB-Bare	21.45	Local
	Gyp-Gyp	21.74	Local
	OSB-Gyp	21.99	Local
	OSB-OSB	23.10	Local
	OSB-OSB	22.84	Local
4	Bare-Bare	19.03	FT
	OSB-Bare	21.99	Local
	Gyp-Gyp	22.39	Local
	OSB-Gyp	21.62	Local
	OSB-OSB	22.26	Local
6	Bare-Bare	13.59	FT
	OSB-Bare	18.01	FT
	Gyp-Gyp	19.94	Local
	OSB-Gyp	20.40	Local
	OSB-OSB	22.38	Local
8	Bare-Bare	12.84	Flexural
	OSB-Bare	15.64	FT
	Gyp-Gyp	21.37	Local
	OSB-Gyp	22.45	Local
	OSB-OSB	23.09	Local

Table 2 – Wall tests, peak load and limit state

Sheathing Configuration	Peak Load (kips)	Limit State	Mean
Bare-Bare	56.33	FT and F	56.33 (56.33/5=11.27)
OSB-Bare	81.57	FT	87.67 (87.67/5=17.53)
	89.21	FT	
	92.23	FT	
Gyp-Gyp	94.07	Local	96.39 (96.39/5=19.28)
	96.66	Local	
	98.44	Local	
OSB-Gyp	103.05	Local	104.92 (104.92/5=20.98)
	105.71	Local	
	105.99	Local	
OSB-OSB	106.04	Local	107.80 (107.8/5=21.56)
	109.55	Local	

2.2 Observed Behavior

The observed limit states for the 8 ft x 8ft walls and the 8 ft long single columns are nearly identical. Only in the Bare-Bare case was some difference observed, as a few of the studs in the full wall test failed in flexural-torsional buckling instead of pure weak-axis flexural buckling. For the shorter length single column tests as the length of the columns gets shorter the global modes are less pronounced and the local mode dominates. In nearly all tests the local buckling failure occurs at the ends of the stud. It is postulated that as the stud is squeezed to fit into the track a large initial imperfection is applied at the end, ultimately triggering failure at this location.

The visually observed global buckling modes are consistent with fixed end conditions. This is likely due to (a) the studs were fully seated in the tracks during assembly and (b) the bearing surface for the track are stiff and level, as they are steel end fixtures. The impact of this condition may be readily observed in Figure 2 where the bare column tests are compared to the values predicted by AISI-S100-07. As can be seen, the assumption of pinned ends (K=1.0) is overly conservative and the ideal fixed end conditions (K=0.5, i.e., K_x=K_y=K_t=0.5) leads to a fine approximation. Note, supplemental analysis by the authors, but not provided here, has shown the importance of applied axial load in closing gaps and restraining warping deformations at the ends, and allowing the full fixity to develop. Also, see LaBoube and Findlay (2007) for more on the impact of stud-to-track gaps on performance. Finally, Figure 2 also provides a comparison between the effective width method of column design utilized in the main Specification of AISI-S100-07 and the Direct Strength Method (DSM) of column design utilized in Appendix 1 of AISI-S100-07. The two methods provide nearly the same result for the studied column without sheathing.

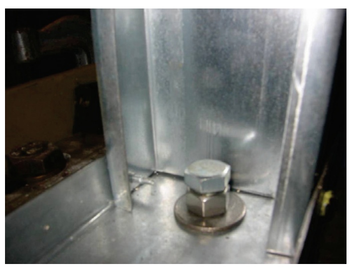

a) Contact stud and track

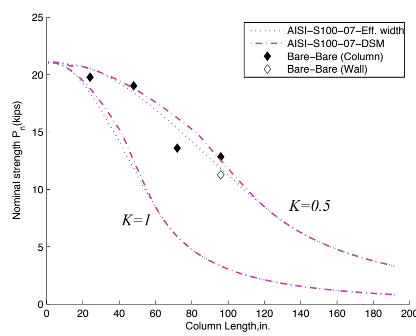

b) Tests and code prediction

Figure 2 – Bare tests and code predictions

3 Estimating restraint supplied by sheathing

With the strength and failure modes established the focus of the work switches to understanding how the sheathing restrains the wall studs. In specific, how the springs of Figure 1e are developed in actual walls is the focus of this section (Section 3), while the impact of the developed springs on the stability of the studs is the focus of Section 4. Finally, the impact on strength is explored in Section 5.

3.1 In-plane lateral (k_x) resistance

Several design models have been developed based on the in-plane stiffness provided by the sheathing to the stud. For instance, Winter's (1960) model assumes that the critical bracing stiffness and strength that sheathing supplies to the stud is derived at the fastener location in direct shear. In essence, arguing that only local deformations must be understood. Simaan and Peköz's (1976) model ignored (simplified) the fact that the shear diaphragm must be resolved through the fasteners and only included flexibility from the diaphragm (the sheathing) itself. Diaphragm stiffness develops as the sheathing itself undergoes shear, which also translates into a lateral resistance at the fastener locations.

Here, it is found that both local and diaphragm resistance exist, and should be included. The importance of including both local and diaphragm stiffness is illustrated with a test on a full-scale wall. Where, instead of sheathing the wall with full boards, OSB strips (2 in. wide) were connected to the studs (Figure 3a). The use of strips negates the shear diaphragm resistance (k_d). The wall failed in flexural buckling at 69.5 kips, Figure 3b, slightly above the bare wall strength, and well below the fully sheathed strength (which fails in local buckling). Sheathing bracing derives from both the local and diaphragm resistance.

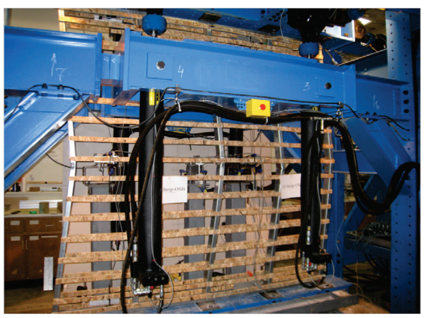

a) Full wall test, strips instead of full boards

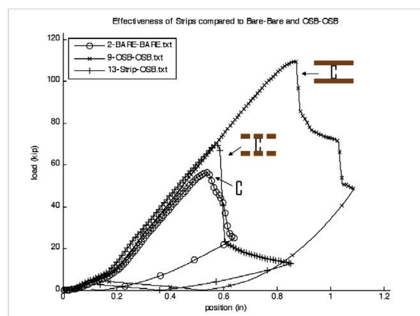

b) Comparison between loading curves

Figure 3 – Effectiveness of strips compared to Bare-Bare and OSB-OSB

To date, existing design methods have provided somewhat contradictory explanations for the manner in which sheathing braces studs, with some methods indicating a strong dependence on stud spacing, others ignoring it altogether. However, if one realizes that the local fastener stiffness is in series with the sheathing diaphragm stiffness then the explanation becomes clear. If local stiffness is low enough (and just as importantly diaphragm stiffness high enough) one will only see the local stiffness in the response and stud and fastener spacing will be largely irrelevant. Conversely, if local stiffness is high enough, say for example from a welded specimen with a steel sheet (and diaphragm stiffness low enough) then only the diaphragm stiffness will be important and stud spacing will be enormously important. Mathematically this may be handled by realizing k_x may be approximated as

$$k_x = 1/(1/k_\ell + 1/k_d) \quad (1)$$

where k_ℓ is determined experimentally, and k_d, as will be shown, can be found using Eq. 2. For bracing strength the local model (and its associated testing) includes the most critical strength limiting failure modes: bearing, tilting, edge pull-out, and screw shear. Failure of the sheathing itself, in shear, and not at the connector location is possible (e.g. in a shear wall), but is generally not an expected failure mode for sheathing only acting as bracing.

In the tests conducted in this work to determine k_ℓ the following variables were taken into account: sheathing type, stud spacing, fastener spacing, edge distance, environmental conditions, and construction flaws. The results provide characterization of the local stiffness and strength that is supplied as the fasteners bear and tilt in a stud-sheathing assembly, Figure 4.

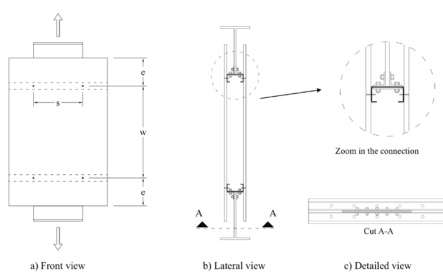

Figure 4 – Test setup design

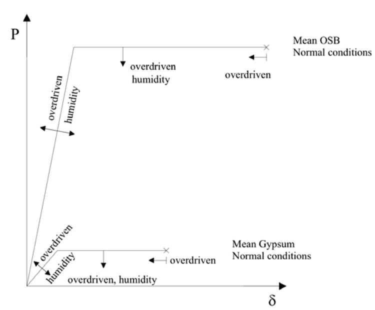

Figure 5 – P-δ of OSB vs. Gypsum

A stylized load-displacement curve, Figure 5, provides a graphical depiction of the average results and dramatically shows the difference between the two sheathing types. As indicated in the figure the impact of humidity and over-driving the fasteners is the same for both sheathing types. Humidity decreases stiffness and strength. Over-driving the fasteners increases stiffness, but decreases strength and deformation capacity.

A condensed summary of the test results is provided in Table 3, where normal conditions refer to w = 24 in.; s = 4, 12, or 20 in.; e = 6 in. (Figure 4); kept for seven days at a temperature of 20C and 65% humidity. The overdriven condition has the same w, s, and e but the screw is overdriven by 1/8''. The humid (saturated) condition has dimensions w = 8 in.; e = 2 in.; and s = 4, 6, 9, 12, and 20 in.; and are kept immersed in water for 7 days.

Table 3 – Condensed summary of test results

		k initial		Pmax		δ @ Pmax	
		mean (kip/in)	coef. variation	mean (kip)	coef. variation	mean (in)	coef. variation
OSB	Normal Conditions	7.08	0.07	0.58	0.03	0.62	0.02
	Overdriven	9.36	0.10	0.41	0.05	0.34	0.27
	Humid (saturated)	6.32	0.10	0.26	0.04	0.51	0.21
Gypsum	Normal Conditions	2.43	0.02	0.09	0.03	0.34	0.13
	Overdriven	3.49	0.14	0.07	0.02	0.15	0.57
	Humid (saturated)	0.24	-	0.02	-	0.42	-

For nominally identical studs, fasteners, and spacing: the lateral stiffness of an OSB sheathed specimen is 3 times greater than gypsum board; the shear capacity in OSB is nearly 7 times greater than gypsum board as the failure mode switches from screw shear to tear out; and the displacement at peak load is 2 times greater in OSB than in gypsum. An additional fifteen tests were conducted comparing plywood samples from Canada and the United States, the results can be found in the report by Vieira and Schafer (2009).

To determine the diaphragm stiffness, k_d, an analytical model was developed based on a plate deformed laterally following a sine-wave curve, Figure 6. In the model the stiffness at a fastener location is the force at the fastener, developed from an integration of the shear stress over the tributary area of the fastener, divided by the deformation, at the fastener location. For sheathing with a low shear modulus or where the panel is wide and short, both typical for the sheathing considered in wall studs, then the stresses are controlled by shear deflections consistent with diaphragm action.

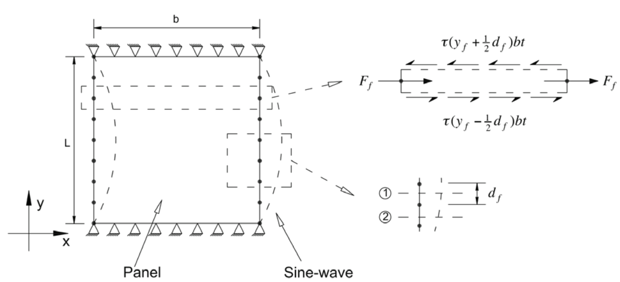

Figure 6 – Plate Model

Vieira and Schafer (2009) provide the full derivation for k_d, that leads to:

$$k_d = \frac{2\pi G t w_{tf}}{L} \cdot \sin\left(\frac{\pi d_f}{2L}\right) \cong \frac{\pi^2 G t w_{tf} d_f}{L^2} \qquad (2)$$

The variables in Eq. 2 are defined in Figure 6 except for shear modulus of the material, G, thickness of the board, t, and tributary width of board, w_{tf}. The primary limitation of Eq. 2 is that the tributary area of fasteners in the field should not be greater than 6 x the tributary area of the fasteners on the edge (perimeter). As the distance between fasteners in the field is increased over this limit the edge fasteners behave as if there were no fasteners in the field and the stiffness goes back to the case of only being connected at the edges. The limitation is not a practical problem since the relation between tributary areas is typically no greater than 4 x (e.g., 6 in. on the edge, 12 in. in the field).

3.2 Rotational (k_ϕ) resistance

As the flange attempts to rotate (due to buckling or other deformations) local tilting of the fastener combined with bending of the sheathing and contact between the flange and sheathing restricts this movement in a manner that may be idealized by a rotational resistance, k_Φ. Rotational tests were performed on the configurations tested herein (same studs, boards, fasteners, and fastener spacing) to check the methodology developed by Schafer et al. (2007), Table 4. Schafer et al. (2010) fully discuss the procedure to find k_Φ, which is represented in Figure 1e and in the paper assumes the nomenclature $k_{\Phi 2}$.

Table 4 – Rotational stiffness tests on 362S162-68 studs
(Stiffness reported in units lbf-in./in./rad)

Test	k_ϕ	$k_{\phi w}$	$k_{\phi c}$	$k_{\phi\text{-}10\%Mmax}$
BBB-GYP-12-6-6-01	68	283	90	77
BBB-GYP-12-6-6-03	78	-	-	67
BBB-GYP-12-6-6-04	79	255	115	79
BBB-GYP-12-6-6-05	58	193	82	52
average	70.8	243.7	95.7	68.9
COV	0.14	0.19	0.18	0.18

Test	k_ϕ	$k_{\phi w}$	$k_{\phi c}$	$k_{\phi\text{-}10\%Mmax}$
BBB-OSB-12-8-6-02	81	288	113	103
BBB-OSB-12-8-6-06	64	201	95	85
BBB-OSB-12-8-6-07	67	212	98	86
BBB-OSB-12-8-6-08	69	243	97	91
average	70.3	236.0	100.8	91.4
COV	0.11	0.17	0.08	0.09

The semi-empirical method developed in Schafer et al. (2007) may be summarized in three equations shown below. Eq. 3 provides the stiffness due to the connection itself, as a function of the stud thickness t (in in.) and steel modulus, E (in ksi). Eq. 4 gives the rigidity provided by the sheathing $(EI)_w$ for different materials and grain orientations (as commonly tabled by APA (2002) and others), and different tributary width, L. Finally Eq. 5 combines both stiffnesses as two rotational springs in series.

$$k_{\phi c} = 0.00035Et^2 + 75 \tag{3}$$

$$k_{\phi w} = (EI)_w/L \tag{4}$$

$$k_\phi = 1/(1/k_{\phi c} + 1/k_{\phi w}) \tag{5}$$

The test values may be compared to the values predicted by the Eq.'s 3-5. For the connection stiffness, Eq. 3 predicts a $k_{\phi c}$ of 123 lbf-in./in./rad, while the mean measured values are 96 lbf-in./in./rad in the gypsum and 101 lbf-in./in./rad in the OSB, as reported in Table 4. Noting that the standard deviation on the original data used to calibrate Eq. 3 was 24 lbf-in./in./rad the measured connection stiffness is 1 standard deviation below the average values, reasonable if not perfect agreement.

For the sheathing stiffness $k_{\phi w}$ is determined by Eq. 4 and the appropriate industry standard $(EI)_w$ values. For gypsum, $k_{\phi w}$ is expected to be between 125 and 333 lbf-in./in./rad (from min and max values reported by GA 2001) compared with an average measured $k_{\phi w}$ of 243 lbf-in./in./rad. The limited rotational capacity of gypsum sheathed specimens is again noted. For OSB Eq. 4 predicts $k_{\phi w}$ of 111 lbf-in./in./rad for stress perpendicular to strength axis (as-tested here) and 541 lbf-in./in./rad for stress parallel to the strength axis, which may be compared with an average measured $k_{\phi w}$ of 236 lbf-in./in./rad. The APA (2004) values are again shown to provide a conservative estimate.

3.3 Out-of-plane lateral (k_y) resistance

Traditionally, when considering sheathing as bracing, the out-of-plane resistance of the sheathing is ignored. In-plane the sheathing restrains weak-axis bending and torsion of the stud, while out-of-plane the sheathing increases major-axis bending stiffness. As flexural-torsional buckling is a common mode in wall studs, this out-of-plane restraint may be influential. The out of plane stiffness that develops from the sheathing under major-axis bending, Figure 7, is the ratio of the force in each fastener to the respective deflection at the fastener. The force at each fastener can be found by the difference in the shear force over the tributary length, thus Eq. 6 gives the out-of-plane stiffness.

$$k_y = \frac{2E_w I\pi^3}{L^3} \cdot \sin\left(\frac{\pi\, d_f}{2L}\right) \tag{6}$$

If the sheathing is fully composite with the stud, then the inertia of the board *I*, takes its upperbound value : $I=bt_s^3/12+bt_s(y_{GC}+t_s/2)^2)$. Or, if no composite action develops then I is simply $bt_s^3/12$ resulting in a lower bound value. Industry tabled values for EI as utilized for $k_{\phi w}$ determination may provide this lower bound approximation.

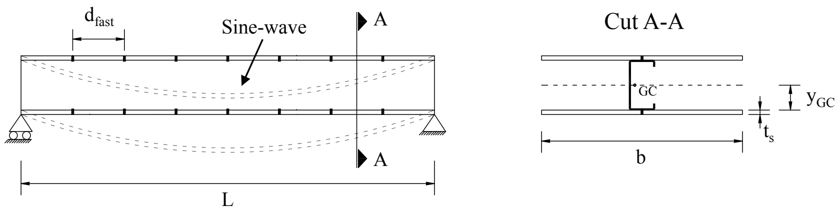

a) Stud under a sine-wave curve on the major axis b) Cross-section

Figure 7 – Analytical model for k_y

4 Stability of sheathing restrained studs

4.1 Unrestrained wall studs

The buckling modes of a pin-pin, unrestrained 362S162-68 SSMA cross-section, the same cross-section used in the columns and walls tests, are provided in the finite strip analysis "signature curve" results of Figure 8. Each buckling mode has an associated buckling half-wavelength (the length of the buckled wave). Understanding how sheathing, or equivalently the springs of Figure 1e, can or cannot change these buckling modes is critical to developing a sheathing braced design method.

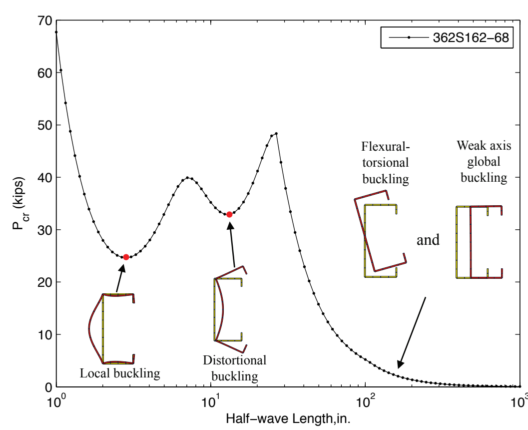

Figure 8 – Buckling curve and modes for pin-pin, unrestrained 362S162-68 SSMA cross-section

4.2 Sheathing restrained wall studs

The following results show how the elastic buckling modes of a cold-formed steel stud are influenced by the sheathing restraint, including different levels of restraint and for dissimilar restraint (different types of sheathing connected to the two flanges). For sheathing on one-side only, i.e. the OSB-Bare tests, Figure 9a compares the results to the unrestrained case. Introduction of the restraint changes the global buckling mode from weak-axis flexure to flexural-torsional buckling, and the resulting flexural-torsional mode is dependent on the level of out-of-plane resistance developed (i.e. lower bound vs. upper bound).

For sheathing on both sides, here the OSB-OSB values are used. Figure 9b compares the buckling results to the unrestrained case. Local buckling is not affected by the restraint, distortional buckling is modestly increased, while global buckling is altered significantly. If only the in-plane resistance is included, at practical lengths, weak-axis flexural buckling is replaced by flexural-torsional buckling. Introduction of the out-of-plane (k_y) resistance increases the flexural-torsional buckling load, and a strong sensitivity to the magnitude of k_y is found. The difference between using the lower bound and upper bound value for k_y is dramatic and should be carefully handled.

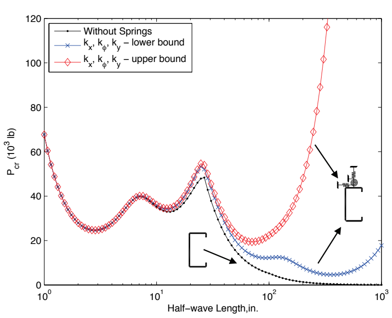

a) Springs on one flange

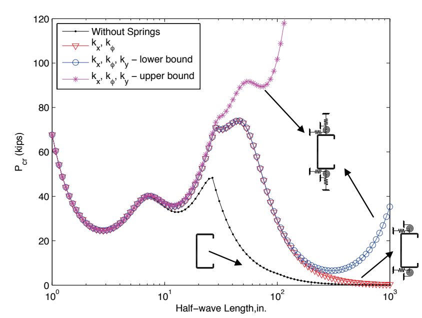

b) Springs on both flanges

Figure 9 – Buckling curves for springs on one flange and both

4.3 Local

Sheathing does not affect local buckling. The sheathing restrains the flange, but local buckling is largely driven by the web anyway. Even theoretically k_x and k_Φ have no influence on local buckling, only k_y. The out-of-plane stiffness, k_y, is derived consistent with global bending resistance and not localized resistance. For local buckling predictions it is recommended to ignore the sheathing.

4.4 Distortional

Distortional buckling is mainly influenced by k_Φ. The AISI-S210-10 (2010) standard provides general methods for finding k_Φ. The rotational stiffness is the recognized means of primary resistance against distortional buckling and is derived and determined in a manner consistent with distortional buckling deformations. The in-plane stiffness, k_x, has little to no influence on distortional buckling in most cases, for very deep webs the additional restraint supplied by k_x could be influential so it may be included if desired. However, the out-of-plane stiffness, k_y, should not be added to k_Φ, in part because k_Φ itself derives from a moment couple that includes k_y at the connector and bearing between the flange and sheathing. Further k_y's deformations are consistent with beam bending, not rotation of the flange. For distortional buckling predictions it is appropriate to use k_x and k_Φ, but ignore k_y.

4.5 Global

Global buckling modes are (a) weak-axis flexure and (b) flexural-torsional buckling. In most cases weak-axis flexure is the lowest mode and thus k_x is critical to this resistance and should be included. For flexural-torsional buckling the torsional component is restrained primarily by the couples created from the k_x springs (but also marginally from the k_Φ springs), while the k_y spring restricts the major axis flexural component. For global buckling predictions at a minimum k_x should be included, but it is appropriate to include k_Φ and k_y as well. In the absence of testing the lowerbound k_y value is the most rational choice.

5 Design Method

5.1 Proposed Methodology

The proposed design methodology is a unique application of the Direct Strength Method (DSM) of AISI-S100-07 Appendix 1. To design via the DSM approach the critical elastic buckling loads for local ($P_{cr\ell}$), distortional (P_{crd}), and global (P_{cre}), are required. Typically these P_{cr} values are for the isolated member cross-section; though work on distortional buckling has shown that if restraint is supplied to a member the P_{cr} (i.e. P_{crd}) can be analyzed with the restraint in place and the increased P_{cr} that results utilized in the DSM strength expressions for prediction of capacity (P_n).

Following the guidance of Sections 4.3-4.5 appropriate restraint (springs) are added to the model of the cross-section to predict $P_{cr\ell}$ and the sheathing-restrained P_{crd} and P_{cre}. The spring stiffness values are selected based on the results of Section 3 and applied to the cross-section by means of foundation stiffness (instead of a discrete spring at the fastener locations). Table 5 presents the spring stiffnesses and sheathing material properties considered.

In addition, and reflecting the findings of Section 2.2, Figure 2b, both pin-pin and fixed-fixed end boundary conditions are considered (for all three buckling modes). The traditional pin-pin models are developed using CUFSM 3.12 (Schafer and Adany (2006)) while the fixed-fixed models are performed in an in-house research version of CUFSM developed by Li and Schafer (2010).

Table 5 – Spring stiffnesses values and material properties considered

Board	k_x (kip/in/in)	k_y-upper bound (kip/in/in)	k_y-lower bound (kip/in/in)	k_ϕ (kip.in/in/rad)	E (ksi)	G (ksi)
OSB	0.2706	0.0355	0.0001710	0.0703	900	45
Gypsum	0.0485	0.0045	0.0000285	0.0708	100	5

5.2 Comparison with tests

As discussed previously, and demonstrated in Figure 2, the bare column (no sheathing) behaves essentially as a member with fixed-fixed end conditions, rather than pin-pin. As a result, both the traditional pin-pin, and upper bound fixed-fixed boundary conditions are explored in the following.

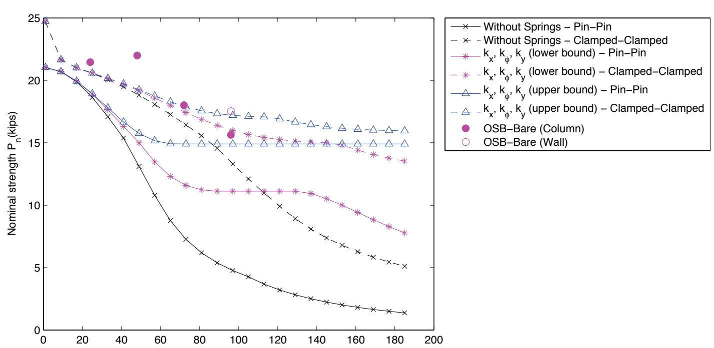

Figure 10 – Bare stud and stud restrained on one side compared to the possible design curves

Figure 10 provides a comparison of design assumptions for the OSB-Bare columns and walls. The tests all failed in a highly restrained version of flexural-torsional buckling. The test data most closely follows the assumption of fixed-fixed end conditions. In fact, up to 72 in. (6 ft), the end conditions are more influential than the sheathing restraint. For longer columns the importance of the sheathing restraint grows significantly. For the fixed-fixed end conditions, the lower bound (noncomposite) approximation for the sheathing contribution to the major–axis bending of the stud (k_y) is sufficiently accurate.

For the columns and walls with sheathing restraint on both sides: Gyp-Gyp, OSB-Gyp and OSB-OSB Figure 11 provides a comparison with potential design assumptions (to provide some clarity the spring values employed in the design curves are those for OSB-OSB). All of the tested columns fail in local buckling, at approximately the same per stud strength. In stark contrast to the case with one-sided sheathing (OSB-Bare) having springs on both flanges dramatically decreases the impact of the end boundary conditions. Even when only considering the in-plane resistance (k_x and k_Φ) this restraint is enough to strongly restrict weak-axis bending and torsion, and up through 72 in. (6 ft) length the end conditions have only a small influence on the result. However, for longer than 72 in. (6 ft) the major-axis bending becomes increasingly important to restrain – either fixed-fixed end conditions or fully composite bending action with the sheathing (k_y upper bound) is required. The assumption of fixed-fixed end conditions and the noncomposite lower bound for k_y is again found to be a good predictor of the behavior. Pin-pin end conditions and only in-plane resistance (in essence the traditional model) is observed to be (a) a conservative predictor, and (b) one that reasonably follows the observed experimental trends.

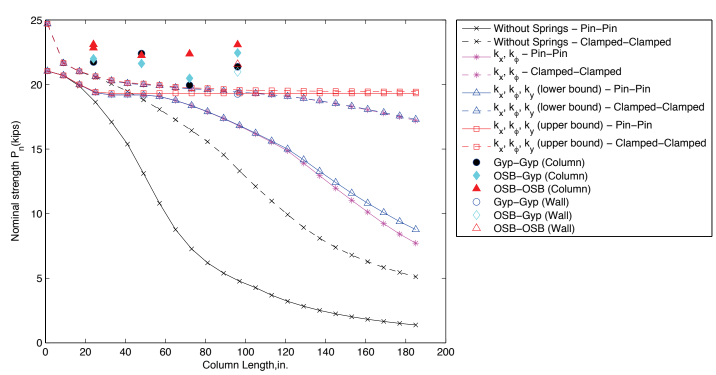

Figure 11 – Studs restrained on both sides compared to possible design curves

Finally, the proposed design method (using DSM and employing fixed-fixed end conditions, k_x and k_ϕ in-plane restraint and the non composite k_y lower bound resistance) is compared to the tests and other currently available design methods. In addition, the actual spring values for OSB and Gypsum board are utilized (per Table 5). The test data compares well with the proposed method and the small differences between OSB-OSB, OSB-Gyp, and Gyp-Gyp are even reflected in the predicted strength, along with the relatively pronounced decrease as a function of length for the one-sided sheathing case: OSB-Bare. The strength prediction is a significant improvement over AISI-S100-01 (essentially the Simann and Peköz 1976 method), Figure 12. The method is also an improvement over AISI-S210-07 both conceptually (AISI-S210-07 simply assumes one fastener is defective and calculates the strength of a column with a length equal to twice the fastener spacing) and in terms of strength prediction.

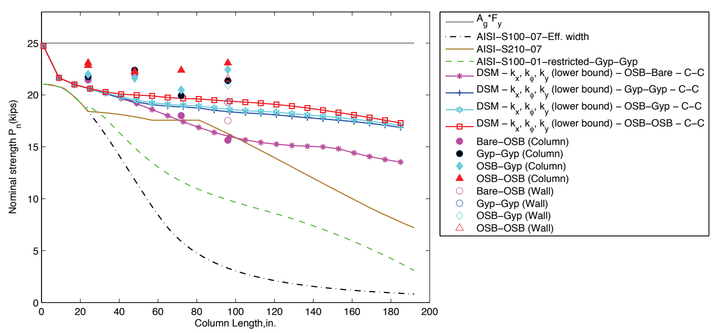

Figure 12 – Test results compared to former, current and proposed design methods

5.3 Fastener demands and future research

A significant and final feature of the proposed design method is still under development: the prediction of fastener demands. As the sheathing braces the studs forces develop at the fastener locations, failure of a fastener means loss of the bracing stiffness, thus the stud strength may be limited by the fastener strength. This may be particularly important for Gypsum sheathing. Preliminary work has been completed to predict the fastener demands as a function of the initial imperfections of the column, for both flexural and flexural-torsional buckling. Verification with nonlinear finite element modeling and development of a design procedure are underway.

6 Conclusions

The Direct Strength Method is shown to be an effective procedure for designing sheathing-braced wall studs. However, the problem must be handled carefully, as the sheathing-based restraint: in-plane, out-of-plane, and rotational must be determined with some care. A combination of experimental and analytical methods is presented herein for determining the restraint (bracing stiffness) associated with sheathing. The end boundary conditions for the studs are found to be fixed-fixed under test conditions, this is particularly important for un-sheathed studs, or studs sheathed on one-side only. For studs sheathed on both sides the end boundary conditions have a much smaller influence on the behavior, this is because the restraint provided by the sheathing largely dominates the response. For wall studs with sheathing on both sides, in the proposed design method, and in the testing, local buckling is the failure mode. Work is now underway to develop predictions of the fastener demands and complete a new procedure for the design of sheathing-braced wall studs covering similar, dissimilar, and one-sided sheathing configurations.

Acknowledgments

The authors gratefully acknowledge the Steel Stud Manufacturers Assoiation and the American Iron and Steel Institute for funding this research, Simpson Strong-Tie for donating the fasteners, and Nickolay Logvinovsky, Lauren Thompson and Hannah Blum for all their aid during the testing. In addition, the work benefitted from the input of the AISI Committee on Framing Standards Project Monitoring Task Group chaired by Nabil Rahman with significant input from Don Allen, Roger Laboube, Sutton Stephens, and Tom Trestain.

References

AISI (1962). Light Gage Cold-Formed Steel Design Manual. American Iron and Steel Institute, New York, NY (now Washington, D.C.)

AISI (2004) North American Specification for the Design of Cold-Formed Steel Structural Members. American Iron and Steel Inst., Wash., D.C.

AISI (2007). North American Standard for Cold-Formed Steel Framing–Wall Stud Design. AISI-S211-07, Am. Iron and Steel Inst., Washington, D.C..

AISI-S210 (2010). "North American Standard for Cold-Formed Steel Framing – Floor and Roof System Design." American Iron and Steel Institute, Washington, D.C., ANSI/AISI-S210-10, 28 pp.

APA (2004) "Panel Design Specification", APA – The Engineered Wood Association.

LaBoube, R.A.; Findlay, P.F. (2007). "Wall Stud-to-Track Gap: Experimental Investigation" Journal of Architectural Engineering, Vol. 13, No.2, June 1, 2007.

Li, Z. and Schafer, B.W. (2010) The constrained finite strip method for general end boundary conditions. Structural Stability Research Council - Proceedings of the 2010 Annual Stability Conference, Orlando, FL, USA, 2010; p 573-591

Miller, T., Peköz, T. (1994). "Behavior of Gypsum-Sheathed Cold-Formed Steel Wall Studs." ASCE, Journal of Structural Eng. 120 (5) 1644-1650.

Schafer, B. W., and Adany, S. (2006), "Buckling analysis of cold-formed steel members using CUFSM: Conventional and constrained finite strip methods." Proc. of the 18th Int'l. Spec. Conf. on Cold-Formed Steel Structures, 39-54.

Shifferaw, Y., Vieira Jr, L. C. M., Schafer, B.W. (2009). "Compression Testing of Single Column Studs with Sheathing Configurations" AISI Progress Report. www.ce.jhu.edu/bschafer/sheathedwalls

Simaan, A. Peköz, T. (1976). "Diaphragm Braced Members and Design of Wall Studs." ASCE, Journal of the Structural Division, 102 (ST1) 77-92.

Vieira Jr, L. C. M., Schafer, B.W. (2009). "Full-scale testing of sheathed cold-formed steel wall stud systems in axial compression" AISI Progress Report. www.ce.jhu.edu/bschafer/sheathedwalls

Winter, G. (1960). "Lateral Bracing of Beams and Columns." ASCE Transactions, Paper No. 3044, per footnote "published in 1958 in the Journal of the Structural Division"